LA-UR-79-657

*conf. 790327--2*

**TITLE:** RF QUADRUPOLE BEAM DYNAMICS

# MASTER

**AUTHOR(S):** Richard H. Stokes
Kenneth R. Crandall
James E. Stovall
Donald A. Swenson

**SUBMITTED TO:**

1979 Particle Accelerator Conference
San Francisco, California

## los alamos
## scientific laboratory
### of the University of California
#### LOS ALAMOS, NEW MEXICO 87545

**DISTRIBUTION OF THIS DOCUMENT IS UNLIMITED**

R. H. Stokes, K. R. Crandall, J. E. Stovall, and D. A. Swenson

Los Alamos Scientific Laboratory
University of California
Los Alamos, New Mexico 87545

## Summary

A method has been developed to analyze the beam dynamics of the radio frequency quadrupole accelerating structure. Calculations show that this structure can accept a dc beam at low velocity, bunch it with high capture efficiency, and accelerate it to a velocity suitable for injection into a drift tube linac.

## Introduction

At present, the proposed use of radio-frequency quadrupole (RFQ) structures for the acceleration of low-velocity ions is receiving increased attention. Of special importance is the structure proposed by Kapchinskii and Teplyakov[1] (K-T) which produces strong focusing electric fields which are spatially continuous along the accelerator axis. The longitudinal accelerating fields which are also present are produced by periodic variations of the radius of the pole tips. To produce the required pole tip potentials several RF systems have been proposed. The predominant effort at LASL is to develop the four-vane resonator operating in the $TE_{210}$ mode. Figure 1 shows a schematic view of this type of resonator.
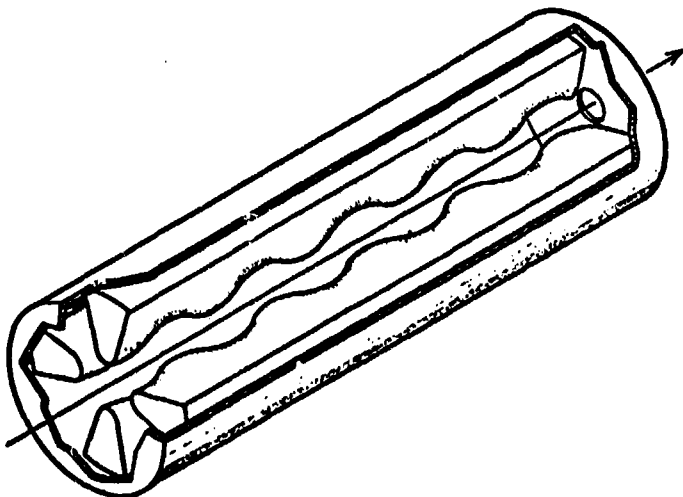


Figure 1.

The expected performance of the RFQ makes it an attractive possibility for use in a variety of accelerator systems. It has been recognized that linac intensity limitations often occur at low velocities where the radial focusing forces from magnetic quadrupoles are weak, and where the longitudinal repulsive forces act for a long time between accelerating gaps. The use of a spatially continuous electric quadrupole force is attractive for the containment of such low-velocity beams. In addition, the longitudinal focusing is greater than in an equivalent drift tube linac for two reasons: (1) for the same frequency the RFQ focusing period is half as long, and (2) for the RFQ the frequency can be higher for a given particle velocity because of the smaller aperture made possible by the strong radial focusing forces.

## Beam Dynamics

Our method of calculating RFQ beam dynamics is based on electric field distributions obtained from the lowest order potential function.[1] The coordinate system has been chosen so that the unit cell encompasses an acceleration gap in a symmetrical manner. The unit cell is $\beta_0\lambda/2$ in length, where $\beta_0 c$ is the synchronous velocity. This is shown in Figure 2.
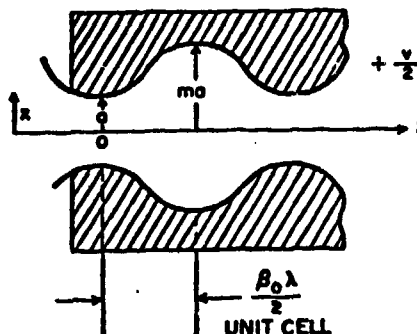


Figure 2.

The electric fields are:

$$E_r = -\frac{XV}{a^2} r \cos 2\psi - \frac{kAV}{2} I_1(kr) \cos kz$$

$$E_\psi = \frac{XV}{a^2} r \sin 2\psi$$

$$E_z = -\frac{kAV}{2} I_0(kr) \sin kz$$

where each component is to be multiplied by the time factor $\sin(\omega t + \phi)$. The quantity $k$ equals $2\pi/\beta_0\lambda$, and A and X are given by:

$$A = \frac{m^2 - 1}{m^2 I_0(ka) + I_0(mka)}$$

and

$$X = 1 - A I_0(ka) \quad .$$

Our notation is the same as in Ref. 1 except that our A equals $4/\pi$ times the quantity $\theta$ used by K-T. The quantity A times V the potential difference between vanes, is the change in the axial potential across one unit cell. Therefore, $E_0$, the average axial field is given by $2AV/\beta_0\lambda$. The quantity X is a measure of the radial focusing strength. It is unity for $m = 1$, and decreases with increasing values of A. For $m = 1.75$ and $ka \ll 1$, both A and X are approximately equal to 0.5.

The hyperbola-like pole tip surfaces[1] which produce the above electric fields in the static approximation are described by the function:

$$x^2 - y^2 = r^2 \cos 2\psi = \frac{a^2}{X}\left[\pm 1 - A I_0(kr) \cos kz\right] \quad .$$

In our resonator design we have characterized the pole tip shapes by using two quantities derived from the above equation. One is the pole tip radius which is obtained through a numerical solution. For example, to describe the pole tip radius in the x-z plane, let

y = 0, take the + sign, and $r$ ... e for the radius which we call $\rho(z)$. The other quantity is $R(z)$, the pole tip radius of curvature in the transverse plane. An expression for $R(z)$ can be derived and then evaluated by using $\rho(z)$ as one input.

Since the radial and longitudinal fields are broadly distributed through the unit cell, the usual gap transformations are not sufficiently accurate to use in describing the particle motion. For this reason we use a smaller transformation interval obtained by dividing the unit cell into n equal parts of length $kz = \pi/n$. These segments extend from $kz = \ell\pi/n$ to $(\ell + 1)\pi/n$. A value of n = 4 or n = 8 has been used in most of our calculations. Initial values of the dynamical quantities x, x', y, y', $\phi$, and W are transformed to final values through each segment. Since we wish to describe the bunching of a dc beam, the description was made valid for all phase angles, and was also made velocity dependent.

## $\phi$ and W Transformations

To transform $\phi$ and W through a segment we have used the relations:

$$\phi_f = \phi_i + \frac{\pi}{n} \varepsilon_1 v + \alpha(v' + \frac{\pi}{n} uw)$$

$$W_f = W_i + Q(u + \varepsilon_1 vw) + \alpha Quvw$$

$$u = I_1 \cos\phi_i + I_3 \sin\phi_i \;, \quad v = I_2 \cos\phi_i + I_4 \sin\phi_i \;,$$

$$w = (1 - \alpha v)^{-1} \;, \quad\quad v' = -I_2 \sin\phi_i + I_4 \cos\phi_i \;,$$

$$Q = \tfrac{1}{2}eVAI_0(kr) \;, \quad\quad \alpha = -Q/2W_s \;,$$

$$\varepsilon_1 = \beta_0/\beta_1 - 1 \;,$$

where $W_s$ is the synchronous energy. The integrals $I_{1-4}$ are functions only of $\ell$ and n. These transformations were obtained from an approximate Hamiltonian function in a manner which insures that the $\phi - W$ phase space is conserved.

## Electric Quadrupole Transformation

The electric quadrupole focusing is represented by a thick lens with the transformation matrices:

$$M_+ = \begin{bmatrix} \cos\theta & \dfrac{\sin\theta}{\theta_0} \\ -\theta_0 \sin\theta & \cos\theta \end{bmatrix}, \quad M_- = \begin{bmatrix} \cosh\theta & \dfrac{\sinh\theta}{\theta_0} \\ \theta_0 \sinh\theta & \cosh\theta \end{bmatrix},$$

where $\quad \theta^2 = \theta_0^2 \left(\dfrac{\beta_0\lambda}{2n}\right)^2 \;,$

and $\quad \theta_0^2 = \dfrac{e}{mc^2\beta^2} \cdot \dfrac{XV}{a^2}|T_f| \;,$

where the second factor is the electric quadrupole gradient averaged over a segment. This factor is the product of the quadrupole amplitude $XV/a^2$ and $T_f$ the focusing transit time function.

$$T_f = \left\langle \sin(\omega t + \phi_i) \right\rangle_{segment}$$

$$= K_A \cos\phi_i + K_B \sin\phi_i$$

where

$$K_A = \frac{n}{6\pi}\left[ \cos\frac{\pi}{n}\ell - \cos\frac{\pi}{n}(\ell + \delta) \right] \;,$$

$$K_B = \frac{n}{6\pi}\left[ \sin\frac{\pi}{n}(\ell + \delta) - \sin\frac{\pi}{n}\ell \right] \;,$$

and $\delta = 1 + \varepsilon_1$. If $T_f$ is positive, the matrix $M_+$ is used to transform x and x' and $M_-$ is used to transform y and y', and conversely if $T_f$ is negative.

## RF Defocus Transformation

The "RF defocus" transformation describes the effect of the second term in the expression for $E_r$. In this case we use a thin lens to transform x – x' and y – y'. For example:

$$\begin{pmatrix} x \\ x' \end{pmatrix}_f = \begin{bmatrix} 1 & 0 \\ \Delta & 1 \end{bmatrix}\begin{pmatrix} x \\ x' \end{pmatrix}_i$$

where $\quad \Delta = -\dfrac{\pi eVAS^2}{2mc^2\beta_0^2\lambda} \cdot J \;,$

and where we have used $I_1(kr) = \tfrac{1}{2}kr$.

$$J = J_A \cos\phi_i + J_B \sin\phi_i \;,$$

$$J_A = J_1 + \varepsilon_1 J_2 + \varepsilon_1^2 J_3 \;,$$

and $\quad J_B = J_4 + \varepsilon_1 J_5 + \varepsilon_1^2 J_6 \;.$

The integrals $J_{1-6}$ are functions only of n and $\ell$.

In addition, we use a conventional form of the adiabatic damping transformation to describe the radial focusing effect of the increase in longitudinal velocity. These four transformations are being incorporated into the PARMILA beam dynamics program in a manner which allows the parameters a, m, and $\phi_s$, the synchronous phase, to be varied as a function of z.

## Applications and Results

There are several possible applications of the RFQ now under consideration at LASL. These include: (1) a high intensity deuteron accelerator being designed for the Hanford Fusion Materials Irradiation Test Facility (FMIT), (2) a high intensity proton accelerator (PIGMI) for use in pion and neutron radiotherapy, and (3) applications to the acceleration of intense heavy ion beams for inertial fusion. To illustrate the properties of the RFQ we will give initial results for the first accelerator above in which the RFQ is to produce a 2 MeV beam for injection into a drift tube linac.

At the present time we have obtained computer results for the longitudinal part of the motion. In the calculations we have injected a dc deuteron beam with an energy of 0.1 MeV into an RFQ which initially has $E_0 = 0$ and $\phi_s = -90°$. $E_0$ and $\phi_s$ were then changed slowly enough so that adiabatic capture occurred with negligible particle loss. This was done by increasing m linearly to reach a final value of approximately 1.9, and by changing $\phi_s$ linearly to reach a final value of $-37°$. The radius parameter a was held constant at 1.0 cm, V was 0.25 MV, and the frequency was 80 MHz. Figure 3 shows the variations of m and $\phi_s$,
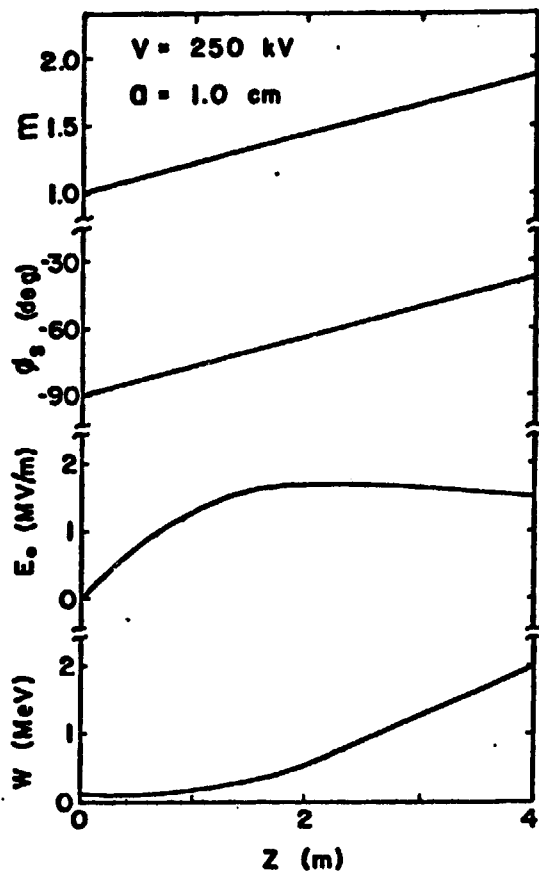
Figure 3.



Figure 4.



Figure 5.

and also shows the accompanying variations of $E_o$ and W. A length of 3.9 m and 109 cells were required to reach the final energy of 2.0 MeV. Figure 4 shows the longitudinal profile of particles passing through this accelerator as calculated by PARMILA. The top graph shows the phase variation of 360 injected particles relative to the synchronous phase, while the lower graph shows the particle energy relative to the synchronous energy. The abscissas are cell numbers. Only one particle fell out of phase and did not reach the final energy, so the capture efficiency was 99.7%. Figure 5 on the left shows the final $\phi - W$ phase space for a low beam current. On the right are results for a 100 ma beam current with longitudinal space charge forces included. The 100 ma beam causes only a small increase in the overall width of phase and energy compared to the low beam calculation.
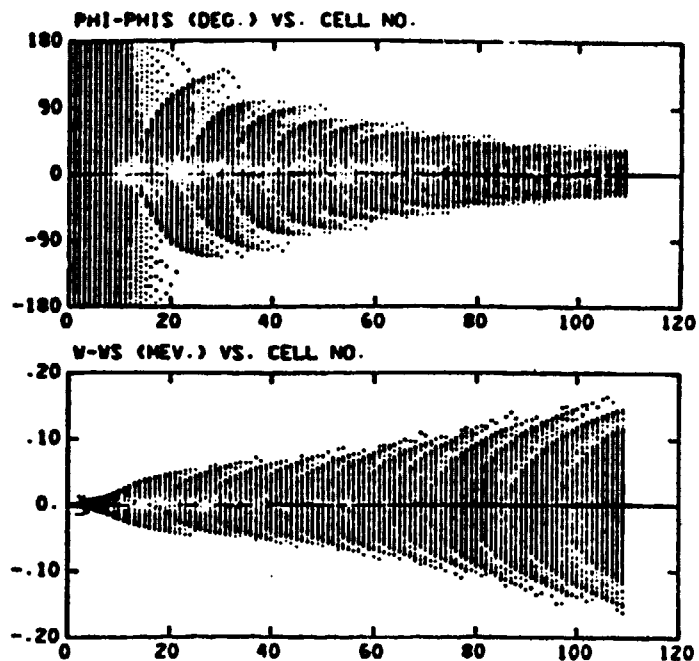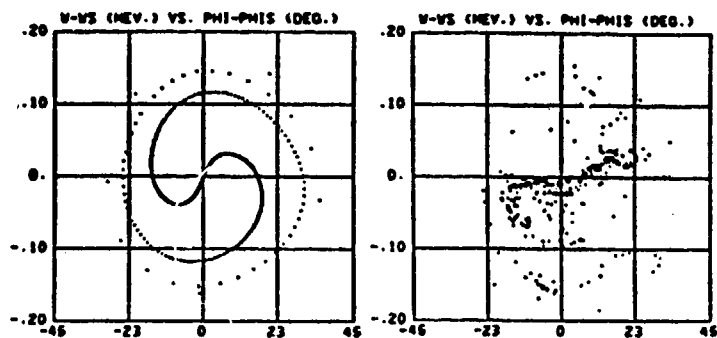
The radial focusing characteristics and the high capture efficiency for low velocity, high intensity beams should make the RFQ an attractive component of many light and heavy ion accelerators.

### References

1.  I. M. Kapchinskii and V. A. Teplyakov, Prib. Tekh. Eksp., No. 2, 19 (1970).